

Supporting information to

**Texture evolution in rhombohedral boron carbide films grown on  
4H-SiC(000 $\bar{1}$ ) and 4H-SiC(0001) substrates by chemical vapor deposition**

*Laurent Souqui<sup>a</sup>, Sachin Sharma, Hans Högberg, Henrik Pedersen*

*Department of Physics, Chemistry and Biology, Linköping University, SE-581 83 Linköping, Sweden*

*<sup>a</sup>Present address: Department of Materials Science and Engineering, University of Illinois at Urbana-Champaign, 1304 W. Green St. MC 246, Urbana, Illinois 61801, USA*

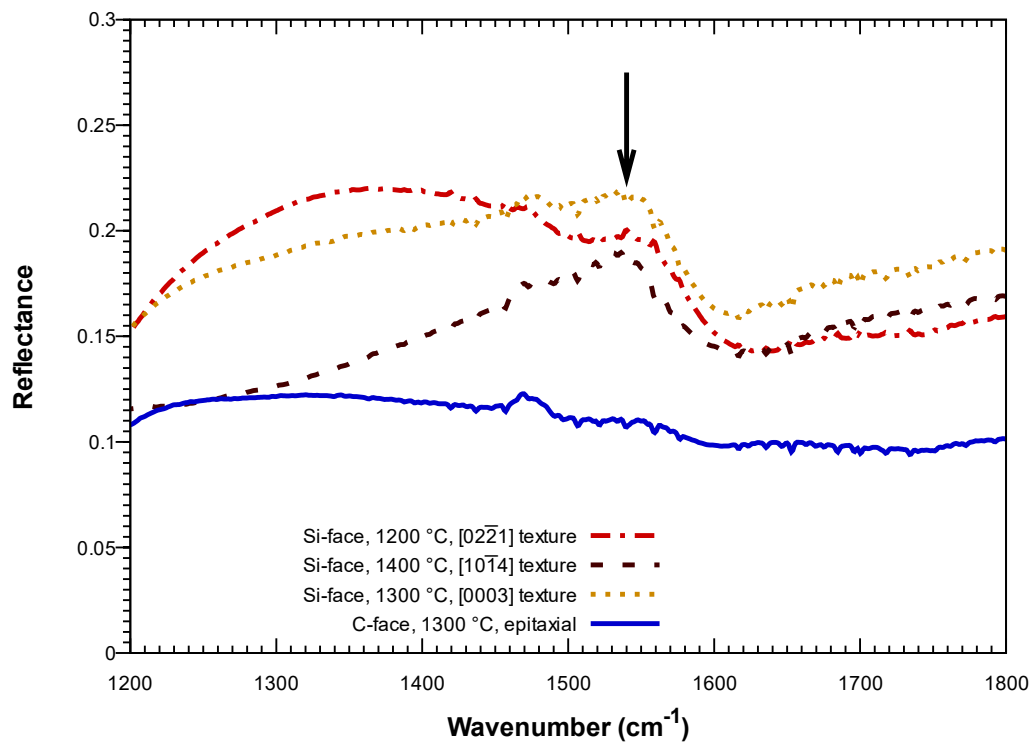


**Fig. S1:** FTIR reflectance spectra of polycrystalline  $r\text{-B}_x\text{C}$  films orientated along  $[02\bar{2}1]$  (dotted yellow curve),  $[10\bar{1}4]$  (dotted-dashed red curve) and  $[0003]$  (dashed brown curve) and epitaxial boron carbide (solid blue curve) around the chain stretching mode around  $1550\text{ cm}^{-1}$  as indicated by the black arrow. The small feature at around  $1470\text{ cm}^{-1}$  originates from the substrate (more clearly visible in Fig. S2).

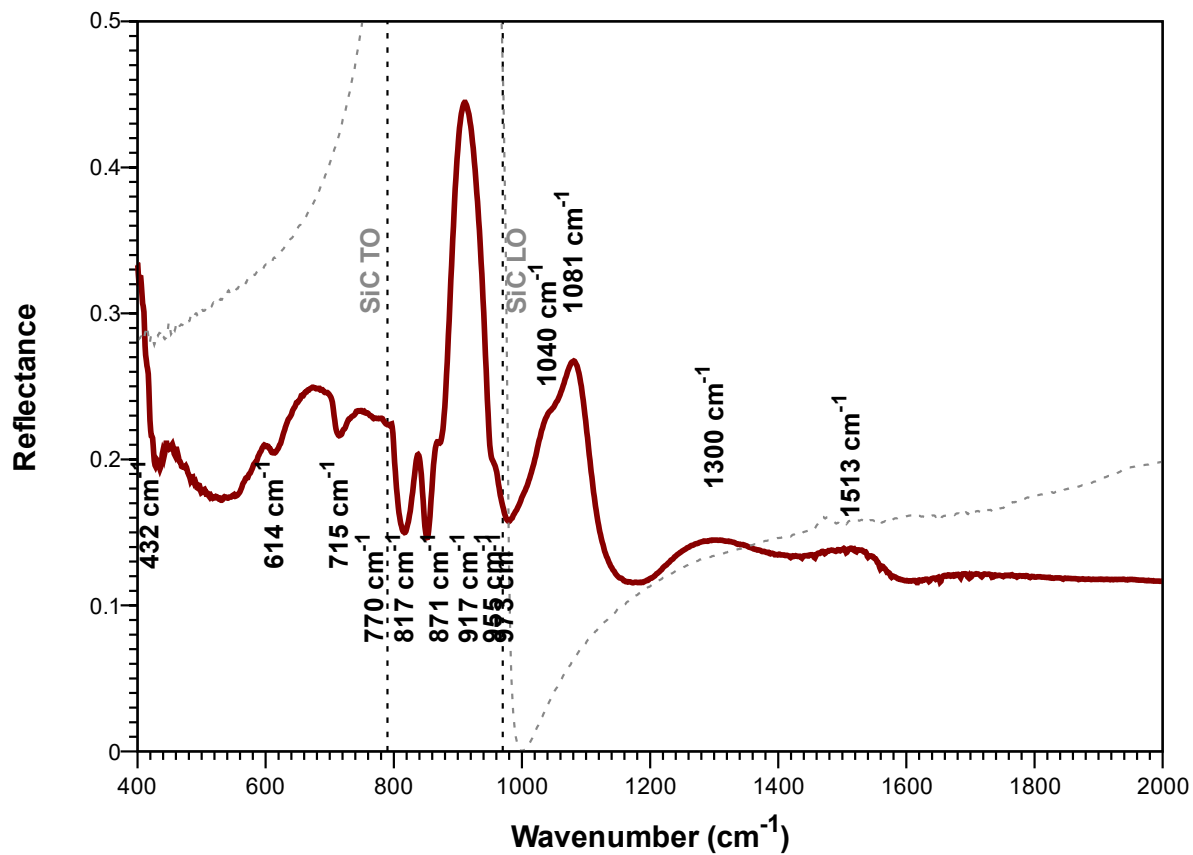


**Fig. S2:** FTIR reflectance spectra of a polycrystalline r-B<sub>x</sub>C film deposited at 1400 °C on Si-face 4H-SiC(0001) (solid red curve) and of the bare 4H-SiC(0001) substrate (dashed grey curve).

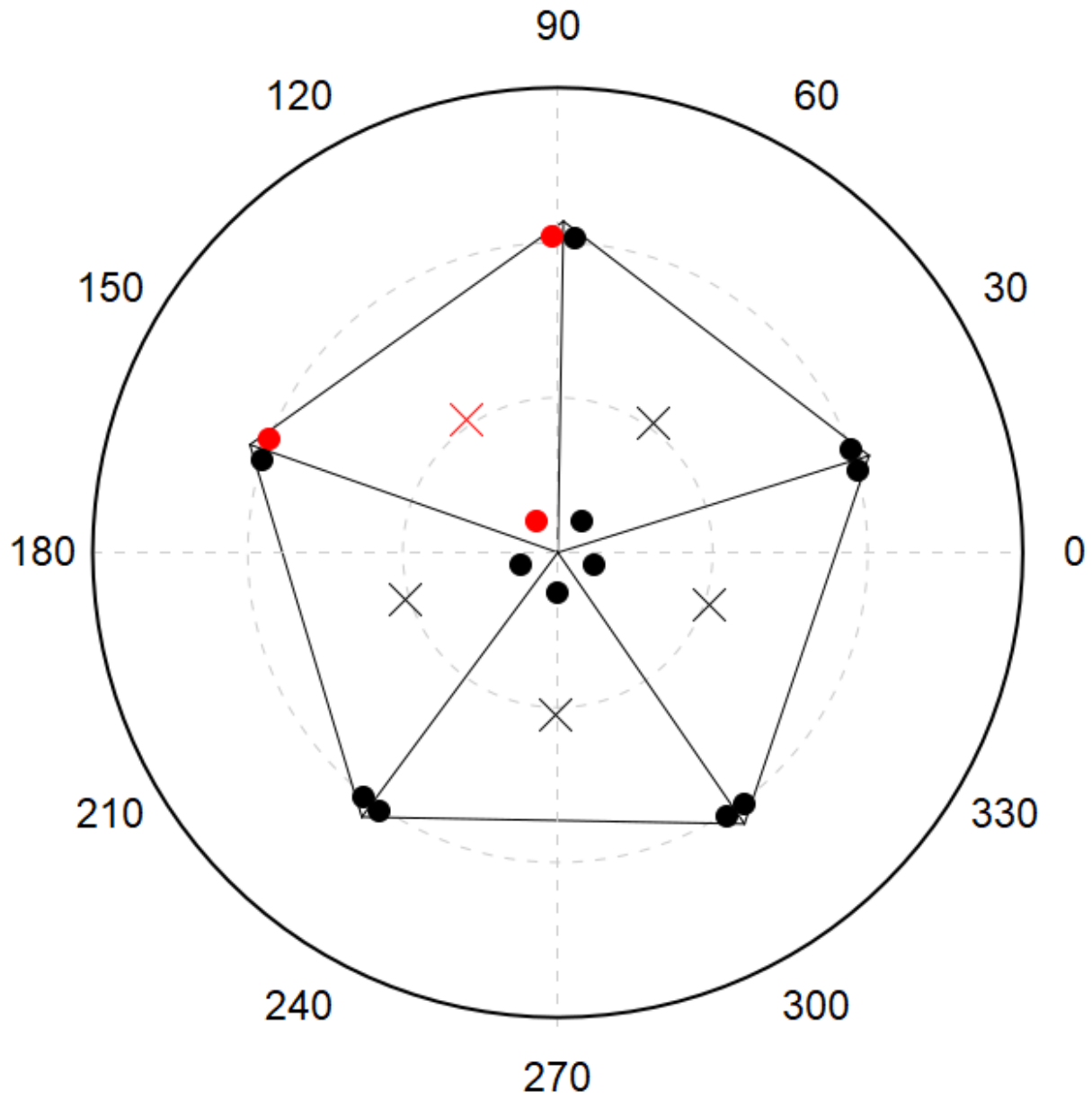


**Fig. S3:** Schematic of a pole figure representing the distribution of poles for one five-fold twinned crystal. The  $(10\bar{1}4)$  poles (red circles) and  $(0003)$  pole (red cross) of an untwinned crystal, and corresponding poles obtained by twinning are shown in black. The pole positions were calculated using the CaRine software.

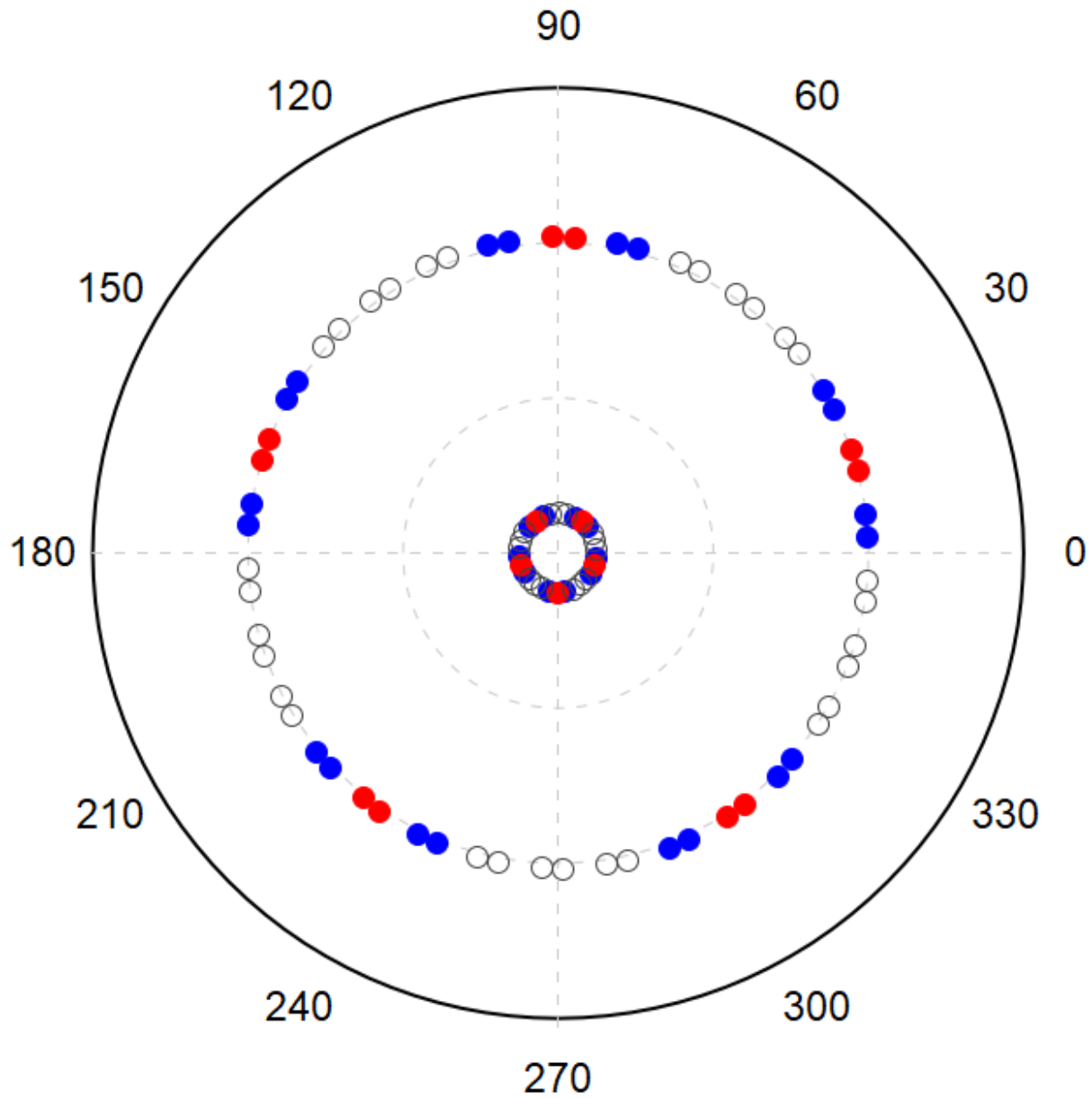


**Fig. S4:** Schematic of a pole figure representing the distribution of  $(10\bar{1}4)$  poles for six five-fold twinned crystals, rotated  $60^\circ$  each from each other, as would be the case on a hexagonal substrate. Here the colours represent a distribution of these crystals so that one orientation (in red) and the ones rotated  $-60^\circ$  and  $+60^\circ$  with respect to that orientation (blue) are the most intense, while the others are weaker. This is comparable to pattern observed in figure 8.